^{68}Ga-pentixafor for PET imaging of chemokine receptor 4 expression in lymphoproliferative diseases and solid tumors

Tingwei Meng Msc,
Qingqing Pan MD,
Yaping Luo MD

Department of Nuclear Medicine, State Key Laboratory of Common Mechanism Research for Major Diseases, Chinese Academy of Medical Sciences and Peking Union Medical College Hospital, Beijing, China.

Keywords: CXCR4 - ^{68}Ga-pentixafor - Lymphoma - Multiple myeloma - Pancreatic cancer

Corresponding author:
Qingqing Pan MD,
Department of Nuclear Medicine, State Key Laboratory of Common Mechanism Research for Major Diseases, Chinese Academy of Medical Sciences and Peking Union Medical College Hospital.
Address: No.1 Shuaifuyuan Wangfujing, Dongcheng District, Beijing, 100730, P. R. China
Tel: 86-10-69154720
pqqelvay@126.com

Yaping Luo MD,
Department of Nuclear Medicine, State Key Laboratory of Common Mechanism Research for Major Diseases, Chinese Academy of Medical Sciences and Peking Union Medical College Hospital.
Address: No.1 Shuaifuyuan Wangfujing, Dongcheng District, Beijing, 100730, P. R. China
Tel: 86-10-69154716
luoyaping@live.com

Received:
13 March 2025
Accepted revised:
26 June 2025

Abstract

Objective: Gallium-68 (^{68}Ga)-pentixafor, a novel positron emission tomography (PET) tracer with high affinity for C-X-C motif chemokine receptor 4 (CXCR4), has recently been introduced in order to assess the CXCR4 expression status in vivo. This study is to investigate the role of ^{68}Ga-pentixafor in detecting various tumors with mice models and to provide references to clinical studies. **Materials and Methods:** Gallium-68-pentixafor and fluorine-18-fluorodeoxyglucose (^{18}F-FDG) PET was performed in opm-2 (lymphoma), daudi (myeloma) and panc1 (pancreatic cancer)-bearing mice. Tumor and background tissue uptake between ^{68}Ga-pentixafor and ^{18}F-FDG PET were compared. Gallium-68-pentixafor PET/computed tomography (CT) was performed in four patients with lymphoma and three patients with multiple myeloma, and ^{18}F-FDG PET/CT was performed as a reference. **Results:** The uptake of ^{68}Ga-pentixafor in background tissues including muscle, liver and kidneys were all lower than those of ^{18}F-FDG. The uptake of ^{68}Ga-pentixafor in the tumors of lymphoma and myeloma-bearing xenografts was comparable or higher than those of ^{18}F-FDG. However, the tumors of panc-1 xenografts had much lower uptake of ^{68}Ga-pentixafor than those in lymphoma and myeloma-bearing mice, and it was also significantly lower than those of ^{18}F-FDG. The high uptake of ^{68}Ga-pentixafor in vivo was confirmed by the high expression of CXCR4 in tumors with immunochemical analysis. Gallium-68-pentixafor PET/CT in patients with marginal zone lymphoma (MZL) and myeloma showed more intense uptake and more extensive involvement than ^{18}F-FDG PET/CT did. Gallium-68-pentixafor and ^{18}F-FDG PET/CT showed comparable uptake in the patient with follicular lymphoma. **Conclusions:** Gallium-68-pentixafor is a promising agent for the evaluation of lymphoproliferative diseases.

Hell J Nucl Med 2025; 28(2): 124-130 *Epub ahead of print: 4 August 2025* *Published online: 30 August 2025*

Introduction

Chemokine receptors form a large family of G-protein coupled receptors that mediate chemotaxis of cells towards a gradient of chemokines. C-X-C motif chemokine receptor 4 (CXCR4) is a transmembrane G-protein-coupled receptor physiologically expressed on T-lymphocytes, B-lymphocytes, monocytes, macrophages, neutrophils and eosinophils as well as hematopoietic stem and progenitor cells in the bone marrow [1]. In pathological conditions, CXCR4 overexpression has been reported in more than 30 different types of cancer crucially involving in tumor dissemination [2], and CXCR4 overexpression has been identified as an adverse prognostic factor of lymphoma, leukemia and solid tumors [3-6].

Gallium-68 (^{68}Ga)-pentixafor, a novel positron emission tomography (PET) tracer with high affinity for CXCR4, has recently been introduced in order to assess the CXCR4 expression status in vivo [7]. In preclinical studies, ^{68}Ga-pentixafor PET/computed tomography (CT) provided images with excellent specificity and contrast in lymphoma and myeloma xenografts [8, 9]. However, the comparison of ^{68}Ga-pentixafor and fluorine-18-fluorodeoxyglucose (^{18}F-FDG) in the distribution of this tracer need further illustrated. Additionally, whether ^{68}Ga-pentixafor could be used to map CXCR4 expression in solid tumors xenografts has not been fully investigated. Thus, we conducted this preclinical study in order to compare the role of ^{68}Ga-pentixafor with ^{18}F-FDG PET in detecting various tumors with mice models and to provide references to further clinical studies.

Materials and Methods

Preparation of ^{68}Ga-pentixafor

The synthesis of ^{68}Ga-pentixafor was performed as described in published articles [10]. In short, 92mL of sodium acetate (1.25M) was added to 1mL of gallium-68 trichloride ($^{68}GaCl_3$) eluent ($^{68}Ga^{3+}$ in 1.0M HCl) obtained from a germanium-68 (^{68}Ge)/^{68}Ga generator (ITG) to adjust the pH to 3.5-4.0. After the addition of a 20μL aliquot (1mg/mL) of DOTA-CPCR4-2 (purchased from CSBio Co.), the mixture was heated to 105°C for 15min. The reaction solution was diluted to 5mL and passed through a preconditioned Sep-Pak C18 Plus Light cartridge (Waters), and the cartridge was eluted with 0.5mL of 75% ethanol to obtain the final product. The radio-chemical purity of the product was analyzed by thin-layer chromatography. The radiochemical purity was always >99%, and the molar activities of the ^{68}Ga-labeled peptides were in the range of 41.3±17.1GBq/μmol. Fluorine-18-FDG was synthesized in-house with an 11MeV cyclotron (CTIRDS 111).

Cell culture and animal model

Opm-2 (lymphoma) and daudi (myeloma) cell lines were grown in Roswell Park Memorial Institute 1640 (RPMI-1640) with 10% fetal bovine serum (FBS), 2mM glutamine, and 100 units/mL penicillin/streptomycin. Panc1(pancreatic cancer) cell lines were incubated in Dulbecco's Modified Eagle Medium (DMEM) medium supplemented with 10% FBS, 2mM glutamine, and 100 units/mL penicillin/streptomycin. All cell lines were maintained in 5% CO_2 at 37°C.

Female nude mice (6-8 weeks, Beijing Vital River Laboratory Animal Technology Co., Ltd.) were subcutaneously injected in the right shoulder with ~5×10^6 daudi cells (or opm-2 or panc1) suspended in 100μL of a 1/1 (v/v) mixture of serum free culture medium and Matrigel (BD Biosciences, Heidelberg, Germany). Once tumors became palpable {100 mm^3 [volume=0.5×long diameter×(short diameter)2]}, approximately 15-21 days post-injection, the animals were employed in the experiments.

In vivo PET study

All mice received ^{68}Ga-pentixafor and ^{18}F-FDG micro PET static scan in two consecutive days. Animals were fasted for 2 hours before scanning. An average of 4.4-15.2MBq ^{68}Ga-pentixafor was injected intravenously into the tail vein of isoflurane anesthetized female daudi (n=4), opm-2 (n=4), and panc1-bearing (n=4) Severe Combined Immunodeficiency mice (SCID mice). Static PET imaging was acquired at 30, 60, 90, 120min p.i. (Inveon micro-PET scanner, Siemens, Germany). Fluorine-18-FDG PET scan was performed at the same time interval after intravenously injection with 8.1-11.5MBq of ^{18}F-FDG. All images were analyzed with the Inveon Research Workspace software, and tumor-to-background ratios were measured.

To fully investigated the advantages of ^{68}Ga-pentixafor comparing to ^{18}F-FDG, PET/CT study in humans was further carried out. Seven patients with lymphoma and multiple myeloma (MM) were included. The study was approved by the institutional review board in Peking Union Medical College Hospital, and written informed consent was obtained from all the patients before PET/CT scan. All PET scans were performed on dedicated PET/CT scanners (Biograph 64 Truepoint TrueV, Siemens, Germany; Polestar m660, SinoUnion, China). For ^{18}F-FDG PET/CT, the patients fasted for at least 6h, and the blood glucose levels were monitored (5.3-7.5mmol/L) before an injection of ^{18}F-FDG (5.55MBq/kg). The PET/CT images (2min/bed) were acquired with an uptake time of 75.0±13.0min (range, 60-83min). For ^{68}Ga-pentixafor PET/CT, imaging was performed (2-3min/bed) with an uptake time of 51.8±13.5 (range, 30-70min) after an injection of 92.5±44.4MBq (range, 55.5-170.2MBq) of ^{68}Ga-pentixafor. The emission scan was obtained from the tip of the skull to the midthigh. All patients underwent unenhanced low-dose CT (120kV; 30-50mAs) for attenuation correction and anatomic reference. For image analysis, all PET/CT scans were read by 2 experienced nuclear medicine physicians (YL and QP). Lesions were visually determined as focally increased tracer retention as compared to surrounding normal tissue. Bone marrow involvement in PET/CT was interpreted as being positive if there was presence of focal lesions with positive PET results, or diffuse bone marrow patterns with uptake higher than liver. The involvement of lymphoma/myeloma, and their highest maximum standardized uptake value (SUVmax) were recorded.

Immunohistochemical staining

The mice were sacrificed after PET imaging and tumor tissues were obtained. For immunohistochemistry, anti-CXCR4 rabbit polyclonal antibody (Abcam) was used. After deparaffinization and rehydration, the slides were placed in a pressure cooker in 0.01M citrate buffer (pH 6.0) and were heated for 7 min. Incubation with the different antibodies was carried out overnight at 4°C. Detection was performed with DAKO envision system according to the manufacturer's protocol.

Statistical analysis

Statistical analyses were done with Medcalc (version 19.6.4) and SPSS Statistics software (version 22.0, IBM SPSS Inc.). Quantitative values were expressed as mean±standard deviation. Comparisons of related metric measurements were performed using Wilcoxon signed-rank test, or Student's t-test was used to compare quantitative data between two paired samples. A P-value <0.05 was considered statistically significant.

Results

Animal studies

Daudi xenografts

The uptake of ^{68}Ga-pentixafor in the tumor of daudi xenografts was increasing over time and clearly delineated 120 mins p.i., which was similar to that of ^{18}F-FDG (uptake of ^{68}Ga-pentixafor vs ^{18}F-FDG: 2.50±4.47% ID/g, vs 2.82±1.82% ID/g, P=0.7859). The uptake of ^{68}Ga-pentixafor in background tissues including muscle, liver and kidneys were all lower than

that of ^{18}F-FDG, especially in muscle 120mins p.i. (^{68}Ga-pentixafor vs ^{18}F-FDG: 0.28±0.10% ID/g, vs 2.36±1.37% ID/g, P= 0.0501). The tumor/muscle, tumor/liver and tumor/ kidneys ratios of ^{68}Ga-pentixafor were all higher than those that of ^{18}F-FDG (Figure 1).

Opm-2 xenografts

The uptake of ^{68}Ga-pentixafor in the tumor of opm-2 xenografts was also increasing over time and clearly delineated 120mins p.i. The tumor uptake showed higher uptake than those of ^{18}F-FDG in the only survival xenograft (the uptake of ^{68}Ga-pentixafor vs ^{18}F-FDG: 5.33±3.09% ID/g vs 4.9% ID/g).

The uptake of ^{68}Ga-pentixafor in background tissues including muscle, liver and kidneys were all lower than those of ^{18}F-FDG, leading to higher tumor/muscle, tumor/liver and tumor/kidneys ratios of ^{68}Ga-pentixafor than those of ^{18}F-FDG. The highest tumor/muscle ratio of ^{68}Ga-pentixafor was delineated at 90mins with the activity uptake of 11.80± 3.23% ID/g comparing to those of ^{18}F-FDG with the activity uptake of 0.69% ID/g. The highest tumor/liver and tumor/ kidneys ratios of ^{68}Ga-pentixafor were delineated at 120 mins with the activity uptake of 4.80±0.53% ID/g and 2.86± 1.22% ID/g, respectively (Figure 2).

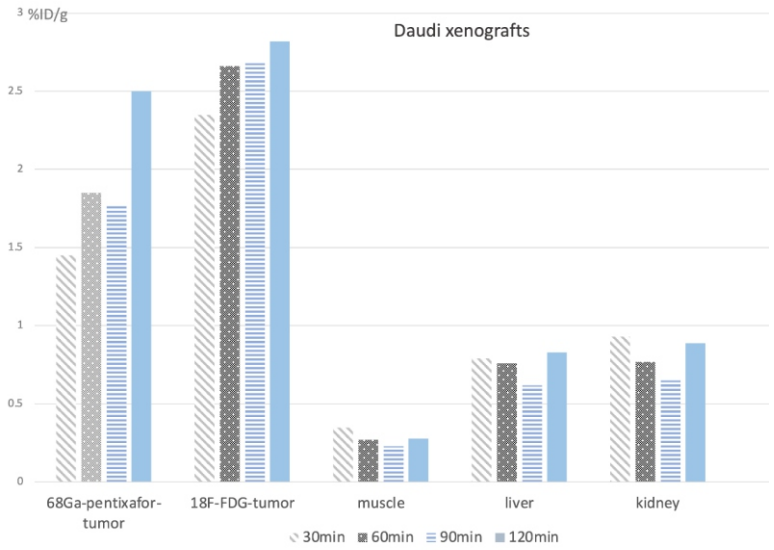

Figure 1. The biodistribution of ^{68}Ga-pentixafor and ^{18}F-FDG at different time points after injection in daudi-bearing mice. The uptake of ^{68}Ga-pentixafor in the tumor of daudi xenografts was increasing over time and clearly delineated 120mins p.i.

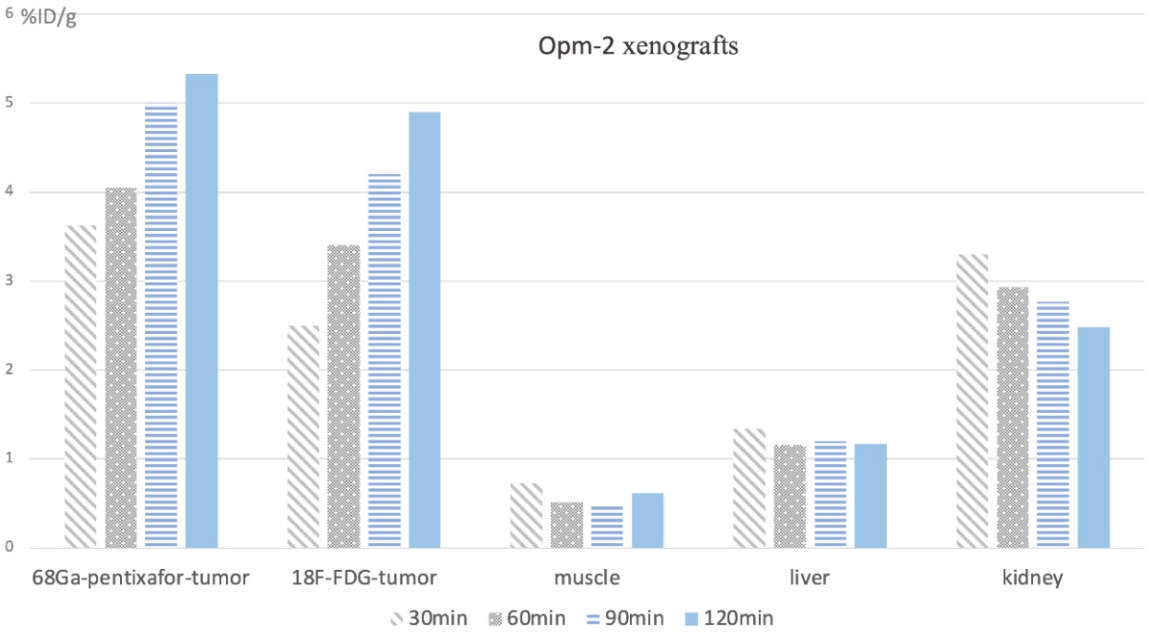

Figure 2. The biodistribution of ^{68}Ga-pentixafor and ^{18}F-FDG after injection at different time points in opm2-bearing mice. The uptake of ^{68}Ga-pentixafor in the tumor of opm-2 xenografts was increasing over time and clearly delineated 120mins p.i..

Panc-1 xenografts

The panc-1 xenografts had much lower uptake of ^{68}Ga-pentixafor than those in daudi and opm-2-bearing mice, and it was also significantly lower than the uptake of ^{18}F-FDG (^{68}Ga-pentixafor vs ^{18}F-FDG: 30mins p.i., 0.46±0.12% ID/g vs 1.18±0.15% ID/g, P=0.0032; 60mins p.i., 0.37±0.14% ID/g vs 1.30±0.18% ID/g, P=0.0008; 90mins p.i., 0.36±0.06% ID/g vs 1.28±0.13% ID/g, P=0.0009; 120mins p.i., 0.41±0.14% ID/g vs 1.35±0.10% ID/g, P=0.0039) (Figure 3).

Immunohistochemical analysis of representative daudi and opm-2 xenograft samples showed intense CXCR4 expression, however it was relatively low in the sample of panc-1-bearing mice. Representative images were shown in Figure 4.

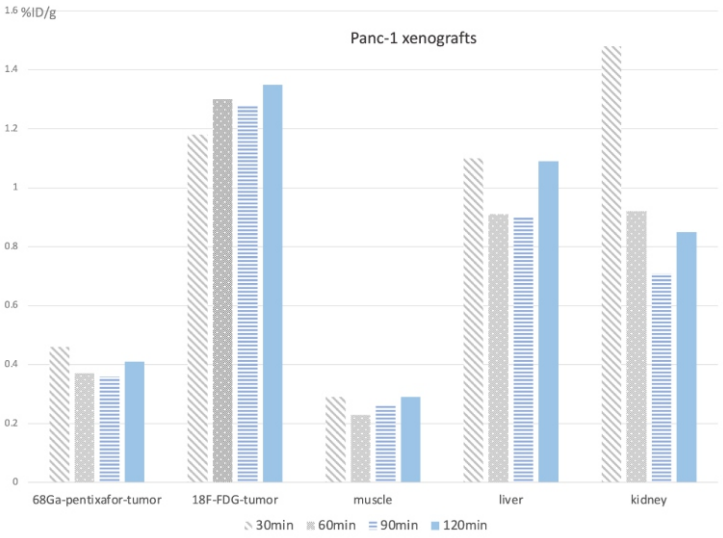

Figure 3. The biodistribution of ^{68}Ga-pentixafor and ^{18}F-FDG after injection at different time points in panc-1-bearing mice. The uptake of ^{68}Ga-pentixafor in panc-1 xenografts was significantly lower than that of ^{18}F-FDG.

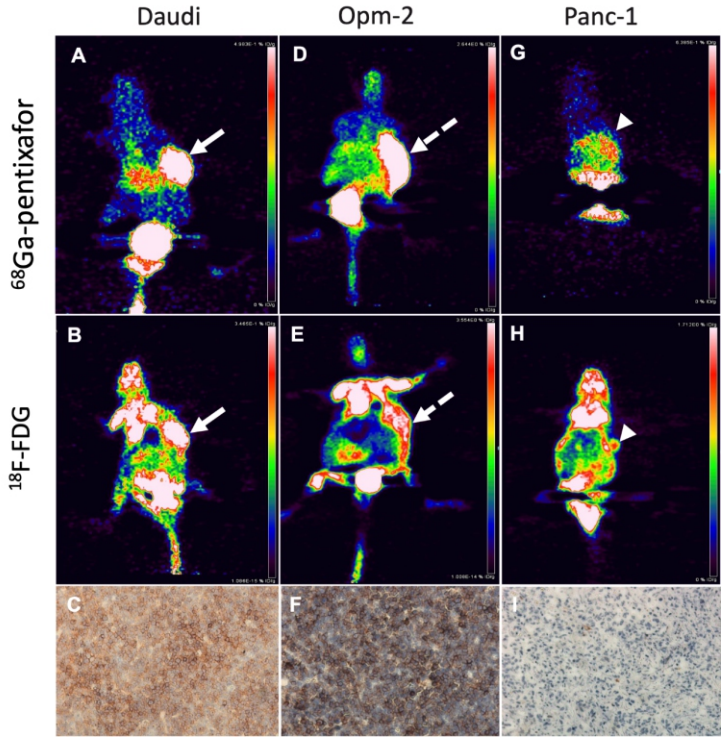

Figure 4. Representative images of three types of xenografts. (A-C) Daudi-bearing mice. Gallium-68-pentixafor (A) and ^{18}F-FDG (B) PET showed intense tracer uptake in tumor on the right shoulder 120min p.i. (white arrows), which was consistent with the high expression of CXCR4 on immunohistochemical analysis (scale bars: 100μm) (C). (D-F) Opm2-bearing mice. The tumor on the right shoulder showed intense uptake of ^{68}Ga-pentixafor PET 120min p.i. (D) and ^{18}F-FDG avidity (E) (white dotted arrows). The immunohistochemical analysis also demonstrated strong CXCR4 expression (scale bars: 100μm) (F). In panc-1-bearing mice, the tumor showed increased uptake of ^{18}F-FDG 120min p.i.(H) but nearly no uptake of ^{68}Ga-pentixafor (G) (white arrow heads). Consistently, CXCR4 expression was low in the tumor sample with immunohistochemical analysis (scale bars: 100 μm) (I)

PET/CT study in humans

Gallium-68-pentixafor PET/CT was further performed in seven patients with histologically proven lymphoma or multiple myeloma. Fluorine-18-FDG PET/CT was performed as comparison (Table 1).

In the three patients with marginal zone lymphoma, ^{68}Ga-pentixafor PET/CT showed superiority to ^{18}F-FDG with more intense uptake and more extensive involvement in bone marrow, lymph nodes, as well as retroperitoneum, kidney, psoas major and dura mater. The SUVmax of ^{68}Ga-pentixafor PET/CT was higher than those of ^{18}F-FDG PET/CT (13.4±4.7 vs. 5.3±5.0, P=0.011). In one patient with follicular lymphoma, ^{68}Ga-pentixafor and ^{18}F-FDG PET/CT both detected lymph nodes involving neck and left inguinal area with similar intensity of tracer uptake (the SUV max, 9.9 vs. 16.3).

In the three patients with multiple myeloma, ^{68}Ga-pentixafor PET/CT were all positive, while ^{18}F-FDG PET/CT were visually negative in two patients and positive in one patient. Gallium-68-pentixafor PET/CT showed more intense and extensive bone marrow involvement than ^{18}F-FDG did. In two patients, ^{68}Ga-pentixafor PET/CT additionally detected focal bone lesions and paramedullary diseases which were not seen in ^{18}F-FDG PET/CT. The SUVmax of ^{68}Ga-pentixafor PET/CT was significantly higher than those of ^{18}F-FDG PET/CT (17.8±2.4 vs. 3.4±1.6, P=0.001). Comparison of maximum intensity projections of PET images were shown in Figure 5.

Discussion

In our study, we evaluated ^{68}Ga-pentixafor as a probe for CXCR4 imaging in xenograft models of lymphoma, myeloma and pancreatic cancer cell lines. The results showed significantly high uptake of ^{68}Ga-pentixafor in lymphoma and myeloma. However, the uptake of ^{68}Ga-pentixafor in pancreatic cancer bearing mice was significantly low.

With its high CXCR4 affinity, ^{68}Ga-pentixafor first demonstrated excellent in vivo pharmacokinetics and highly specific accumulation in CXCR4-positive cell lines of small cell lung cancer [11]. In addition, Wester et al. (2015) found that CXCR4 expression correlated with lymphoma cellular uptake, and ^{68}Ga-pentixafor PET/CT studies showed excellent imaging properties in lymphoma-bearing mice [4]. In patient studies, ^{68}Ga-pentixafor PET/CT showed excellent tumor uptake in diffuse large B-cell lymphoma and aggressive T-cell lymphoma [4]. Our study showed consistent results with previous studies of high uptake of ^{68}Ga-pentixafor in lymphoma tumors [12-16]. Furthermore, ^{68}Ga-pentixafor PET/CT showed superior imaging characteristics to ^{18}F-FDG in three patients with MZL, with more intense and extensive lesions detected. Staging of marginal zone lymphoma is challenging with ^{18}F-FDG PET/CT because marginal zone lymphoma does not usually present with increased glycolysis and may have heterogeneous metabolic behavior [17, 18]. Therefore, it's suggested that ^{68}Ga-pentixafor PET/CT may have the potential to be used in the evaluation of lymphomas, particularly in those types of lymphoma with low ^{18}F-FDG avidity.

Fluorine-18-FDG PET/CT has an impact on the work up of MM. However, the false-negative ^{18}F-FDG uptake [19-22] due

Table 1. *Patients' clinical characteristics and PET/CT results.*

Age/sex	Tumor type	Involvement	SUVmax of PET/CT	
			^{68}Ga-pentixafor	^{18}F-FDG
59/M	MZL (Ann Arbor IV)	Bone marrow, lymph node	6.7	2.7
51/M	MZL (Ann Arbor IV)	Bone marrow, lymph node	11.0	2.6
65/ F	MZL (Ann Arbor IV)	Retroperitoneum, kidney, psoas major, dura mater	12.5	5.2
59/M	FL (Grade 1-2)	Lymph node	9.9	16.3
74/M	MM (LC-λ, ISS III)	Bone marrow	15.5	2.3
49/ F	MM (IgA-κ, ISS III)	Bone marrow	20.3	5.2
61/M	MM (LC-κ, ISS III)	Bone marrow	17.7	2.7

MZL=marginal zone lymphoma, FL= follicular lymphoma, MM= multiple myeloma, LC=light chain, ISS= International Staging System.

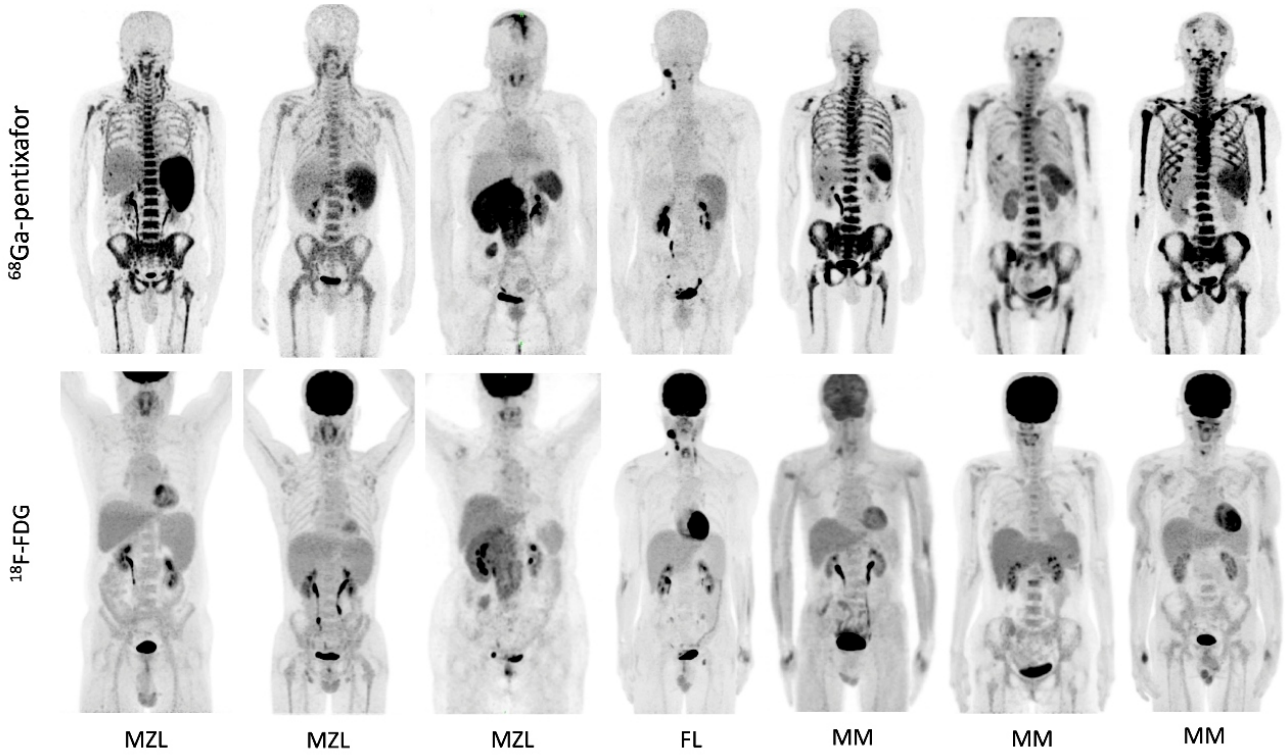

Figure 5. Individual comparison of lymphoproliferative diseases shown on ^{68}Ga-pentixafor and ^{18}F-FDG PET/CT. Gallium-68-pentixafor PET showed obviously higher intensity than ^{18}F-FDG uptake in marginal zone lymphoma (MZL) and multiple myeloma (MM) with more intense uptake in involved bone marrow, lymph nodes, as well as extranodal lesions. In follicular lymphoma (FL), ^{68}Ga-pentixafor and ^{18}F-FDG PET detected involvement of cervical and inguinal lymph nodes with comparable uptake of both tracer.

to the loss of hexokinase-2 expression in MM [23] hampers the assessment of the extent of disease and staging of MM with ^{18}F-FDG PET/CT. According to our study, ^{68}Ga-pentixafor demonstrated high accumulation and tumor to background ratio in MM tumors in vivo, which was consistent with the previous study [24-27]. The high expression of CXCR4 on tumor cell surface revealed by immunohistochemical analysis was considered to be correlated with the high uptake of ^{68}Ga-pentixafor in our small animal PET. This correlation was also confirmed by the previous study using flow cytometric quantification of cell surface CXCR4 expression on MM tumors [21]. We further applied ^{68}Ga-pentixafor PET/CT in patients with MM. In three patients with advanced MM, ^{68}Ga-pentixafor PET/CT scans revealed extensive MM involvement, whereas all ^{18}F-FDG PET/CT scans were rated visually negative. These encouraging results suggested ^{68}Ga-pentixafor PET/CT may overcome the shortcomings of ^{18}F-FDG in the evaluation of MM patients.

In contrast to the high tracer avidity in lymphoma and MM, ^{68}Ga-pentixafor showed very low uptake in panc1-bearing mice, and it also showed significantly lower uptake than ^{18}F-FDG in our study. The immunohistochemical analysis confirmed the low expression of CXCR4 on panc1 cells. As to solid tumors, previous literatures showed very high tracer uptake (SUVmax >12) was found in adrenocortical carcinoma, adrenocortical adenoma, and small cell lung cancer [28], however 37.5% of the patients with pancreatic cancer were negative with ^{68}Ga-pentixafor [29]. This heterogeneous uptake of ^{68}Ga-pentixafor in different types of solid tumors should be further investigated especially when using ^{68}Ga-pentixafor PET/CT as an approach for patient selection for CXCR4-targeted therapies.

In conclusion, ^{68}Ga-pentixafor PET showed high uptake in lymphoma and MM, and may be a promising method for assessing lymphoproliferative diseases. However, pancreatic cancer may not be indicated for ^{68}Ga-pentixafor PET.

The authors declare that they have no conflicts of interest.

Ethics approval and consent to participate

We performed this study in compliance with the 1964 Helsinki Declaration and its later amendments and federal laws in China. The study was approved by the institutional review board of PUMCH (IRB protocol # ZS-1810) and registered at Clinicaltrial.gov (NCT 04514614). All patients signed written informed consent for participation in this study.

Funding

This study has received funding by National High Level Hospital Clinical Research Funding (2022-PUMCH-A-127, 2022-PUMCH-B-070, 2022-PUMCH-B-071) and Peking Union Medical College Hospital Talent Cultivation Program (Categoty C, UBJ10707).

Bibliography

1. Teicher BA, Fricker SP. CXCL12 (SDF-1)/CXCR4 pathway in cancer. *Clin Cancer Res* 2010; 16: 2927-31.
2. Domanska UM, Kruizinga RC, Nagengast WB et al. A review on CXCR4/CXCL12 axis in oncology: no place to hide. *Eur J Cancer* 2013; 49: 219-30.
3. Scotton CJ, Wilson JL, Scott K et al. Multiple actions of the chemokine CXCL12 on epithelial tumor cells in human ovarian cancer. *Cancer Res* 2002; 62: 5930-8.
4. Lapa C, Lückerath K, Kleinlein I et al. ^{68}Ga-Pentixafor-PET/CT for Imaging of Chemokine Receptor 4 Expression in Glioblastoma. *Theranostics* 2016; 6: 428-34.
5. Müller A, Homey B, Soto H et al. Involvement of chemokine receptors in breast cancer metastasis. *Nature* 2001; 410: 50-6.
6. Burger JA, Peled A. CXCR4 antagonists: targeting the microenvironment in leukemia and other cancers. *Leukemia* 2009; 23: 43-52.
7. Herrmann K, Lapa C, Wester HJ et al. Biodistribution and radiation dosimetry for the chemokine receptor CXCR4-targeting probe ^{68}Ga-pentixafor. *J Nucl Med* 2015; 56: 410-6.
8. Philipp-Abbrederis K, Herrmann K, Knop S et al. In vivo molecular imaging of chemokine receptor CXCR4 expression in patients with advanced multiple myeloma. *EMBO Mol Med* 2015; 7: 477-87.
9. Wester HJ, Keller U, Schottelius M et al. Disclosing the CXCR4 expression in lymphoproliferative diseases by targeted molecular imaging. *Theranostics* 2015; 5: 618-30.
10. Pan Q, Luo Y, Zhang Y et al. Preliminary evidence of imaging of chemokine receptor-4 targeted PET/CT with ^{68}Ga pentixafor in non-Hodgkin lymphoma: comparison to ^{18}F-FDG. *EJNMMI Res* 2020; 10: 89.
11. Gourni E, Demmer O, Schottelius M et al. PET of CXCR4 expression by a ^{68}Ga-labeled highly specific targeted contrast agent. *J Nucl Med* 2011; 52: 1803-10.
12. Pan Q, Luo Y, Cao X et al. Posttreated POEMS Syndrome With Concurrent Follicular Lymphoma Revealed by ^{18}F-FDG and ^{68}Ga-Pentixafor PET/CT. *Clin Nucl Med* 2020; 45: 220-2.
13. Luo Y, Cao X, Pan Q et al. ^{68}Ga-Pentixafor PET/CT for Imaging of Chemokine Receptor 4 Expression in Waldenström Macroglobulinemia/Lymphoplasmacytic Lymphoma: Comparison to ^{18}F-FDG PET/CT. *J Nucl Med* 2019; 60: 1724-9.
14. Pan Q, Cao X, Luo Y et al. Chemokine Receptor 4-Targeted ^{68}Ga-Pentixafor PET/CT in Response Assessment of Waldenström Macroglobulinemia/Lymphoplasmacytic Lymphoma: Comparison to ^{18}F-FDG PET/CT. *Clin Nucl Med* 2021; 46: 732-7.
15. Pan Q, Cao X, Luo Y et al. Semi-quantitative measurements of chemokine receptor 4-targeted ^{68}Ga-pentixafor PET/CT in response assessment of Waldenström macroglobulinemia/lymphoplasmacytic lymphoma. *EJNMMI Res* 2021; 11: 110.
16. Pan Q, Luo Y, Zhang Y et al. Preliminary evidence of imaging of chemokine receptor-4-targeted PET/CT with ^{68}Ga-pentixafor in non-Hodgkin lymphoma: comparison to ^{18}F-FDG. *EJNMMI Res* 2020; 10: 89.
17. Albano D, Bosio G, Giubbini R, Bertagna F. ^{18}F-FDG PET/CT and extragastric MALT lymphoma: role of Ki-67 score and plasmacytic differentiation. *Leuk Lymphoma* 2017; 58: 2328-34.
18. Albano D, Durmo R, Treglia G et al. ^{18}F-FDG PET/CT or PET Role in MALT Lymphoma: An Open Issue not Yet Solved-A Critical Review. *Clin Lymphoma Myeloma Leuk* 2020; 20: 137-46.
19. Zamagni E, Nanni C, Patriarca F et al. A prospective comparison of ^{18}F-fluorodeoxyglucose positron emission tomography-computed tomography, magnetic resonance imaging and whole-body planar radiographs in the assessment of bone disease in newly diagnosed multiple myeloma. *Haematologica* 2007; 92: 50-5.
20. Spinnato P, Bazzocchi A, Brioli A et al. Contrast enhanced MRI and ^{18}F-FDG PET-CT in the assessment of multiple myeloma: a comparison of results in different phases of the disease. *Eur J Radiol* 2012; 81: 4013-8.
21. Philipp-Abbrederis K, Herrmann K, Knop S et al. In vivo molecular imaging of chemokine receptor CXCR4 expression in patients with advanced multiple myeloma. *EMBO Mol Med* 2015; 7: 477-87.
22. Nanni C, Zamagni E, Farsad M et al. Role of ^{18}F-FDG PET/CT in the assessment of bone involvement in newly diagnosed multiple myeloma: preliminary results. *Eur J Nucl Med Mol Imaging* 2006; 33: 525-31.
23. Rasche L, Angtuaco E, McDonald JE et al. Low expression of hexokinase-2 is associated with false-negative ^{18}F-FDG-positron emission tomography in multiple myeloma. *Blood* 2017; 130: 30-4.
24. Lapa C, Schreder M, Schirbel A et al. ^{68}Ga-Pentixafor-PET/CT for imaging of chemokine receptor CXCR4 expression in multiple myeloma - Comparison to ^{18}F-FDG and laboratory values. *Theranostics* 2017; 7: 205-12.
25. Pan Q, Luo Y, Cao X et al. Multiple Myeloma Presenting as a Superscan on ^{68}Ga-Pentixafor PET/CT. *Clin Nucl Med* 2018; 43: 462-3.
26. Pan Q, Cao X, Luo Y et al. Chemokine receptor-4 targeted PET/CT with ^{68}Ga-Pentixafor in assessment of newly diagnosed multiple myeloma: comparison to ^{18}F-FDG PET/CT. *Eur J Nucl Med Mol Imaging* 2020; 47: 537-46.
27. Pan Q, Luo Y, Cao X, Li J. ^{68}Ga-Pentixafor PET/CT Improves the Detection of Recurrent Myeloma in the Temporal Bone Masked by the Physiological ^{18}F-FDG Uptake of the Brain and Extraocular Muscles. *Clin Nucl Med* 2022; 47: e348-e50.
28. Buck AK, Haug A, Dreher N et al. Imaging of C-X-C Motif Chemokine Receptor 4 Expression in 690 Patients with Solid or Hematologic Neoplasms Using ^{68}Ga-Pentixafor PET. *J Nucl Med* 2022; 63: 1687-92.
29. Dreher N, Hahner S, Fuß CT et al. CXCR4-directed PET/CT with ^{68}Ga-pentixafor in solid tumors-a comprehensive analysis of imaging findings and comparison with histopathology. *Eur J Nucl Med Mol Imaging* 2024; 51: 1383-94.